Biochemical and Biophysical Research Communications **256,** 156–161 (1999)
Article ID bbrc.1998.9437, available online at http://www.idealibrary.com on IDEAL®

The Solution Structure of Heregulin-α and a N-Terminal Mutant with Suppressed Activity

Marc Adler*,[1] and Stewart A. Thompson†
**Department of Pharmaceutical Discovery and †Department of Biodiscovery, Berlex Biosciences, Richmond, California 94804*

Received September 1, 1998

NMR spectroscopy is used to compare the structure of the EGF-like domain of heregulin-α and HT1, a mutated form of heregulin-α with significantly reduced activity. HT1 is a chimeric protein that has the first seven residues of transforming growth factor-α and the sequence of heregulin-α from the first cysteine through the next 58 residues. The results demonstrate that both proteins share the same fold, including the triple stranded β-sheet formed by the N-terminus and the B-loop. Analysis of the chemical shifts indicates that there are perturbations to the side chain packing of the β-sheet. The observed changes in the chemical shifts show an interesting correspondence to the results from the homologue scan presented in the previous paper. These results indicate that the binding epitope for the native receptor extends across the β-sheet and includes residues Leu[179], Lys[181], Leu[209], and Lys[211].

Site specific mutageneses is a powerful tool for determining which amino acids are important for the function of a protein. The previous paper (1) uses this technique to map out the binding determinants in heregulin-α (HRGα). This paper extends the work of previous investigators who have used this technique (2, 3). Unfortunately, the results from the mutageneses studies are still open to interpretation. Specifically, let us examine the data from the HT1 mutant in the previous paper. In this mutant, the first five residues of heregulin-α, SHLVK, are replaced by the N-terminal fragment from transforming growth factor-α (TGFα), VVSHFND. The mutation results in more than a thousand fold loss in binding activity. The simplest interpretation of the data is that the N-terminus of HRGα is a critical part of the binding determinant.

There is, however, a second interpretation. The observed loss of activity could result from changes in the protein structure. NMR studies have shown that the N-terminus of HRGα is part of triple stranded β-sheet that includes the B-loop (4, 5, and this paper). However, the N-terminus TGFα does not form any compact structure (6). The substitution of TGFα sequence into HRGα may cause the β-sheet structure to unfold. The N-terminus may only be important in maintaining the proper structure and may play no direct role in the binding of HRGα to its receptor.

The work presented here clearly demonstrates that the HT1 mutant of HRGα has the same global fold as the wild type protein. However, the NMR data do indicate that there are perturbations to the packing of the side chains in the triple stranded β-sheet. The results show an interesting correspondence between these structural changes and the results from the homologue scanning mutagenesis presented in the previous paper (1). The data indicate that the epitope that determines binding specificity for the heregulin-α receptor extends across the entire β-sheet and includes both the N-terminus and parts of the B-loop.

MATERIALS AND METHODS

Preparation of recombinant proteins. The preparation of proteins used for this research is described in the preceding article (1).

NMR measurements. All NMR measurements were made on a Bruker AMX 500. The samples were dissolved in 94% H2O and 6% D_2O. The pH was adjusted to 3.1 ± 0.1. No buffers or salts were used. The sample concentrations were approximately 1.5 mM for both heregulin-α and HT1. ^{1}H NMR spectra were acquired at 8°C and 25°C using the same techniques as Adler et al. (7) except that water

[1] To whom correspondence should be sent: Berlex Biosciences, 15049 San Pablo Avenue, Richmond, CA 94804. Fax: 510-262-7844. E-mail: marc_adler@berlex.com.

Abbreviations used: A-loop, residues 182-190 in heregulin-α; B-loop, residues 196-211 in heregulin-α; C-loop, residues 212-221 in heregulin-α; HRGα, the EGF-like domain heregulin-α; NMR, nuclear magnetic resonance; HT1, a chimeric protein that has the first seven residues of transforming growth factor-α and the sequence of heregulin-α from the first cysteine through the next 58 residues; NOE, nuclear Overhauser effect (an NOE peak between two protons indicates a separation of less than 5Å); NOESY, two-dimensional nuclear Overhauser enhancement spectroscopy; ppm, parts per million; RMSd, root mean squared deviation; TGFα, transforming growth factor-α.

0006-291X/99 $30.00

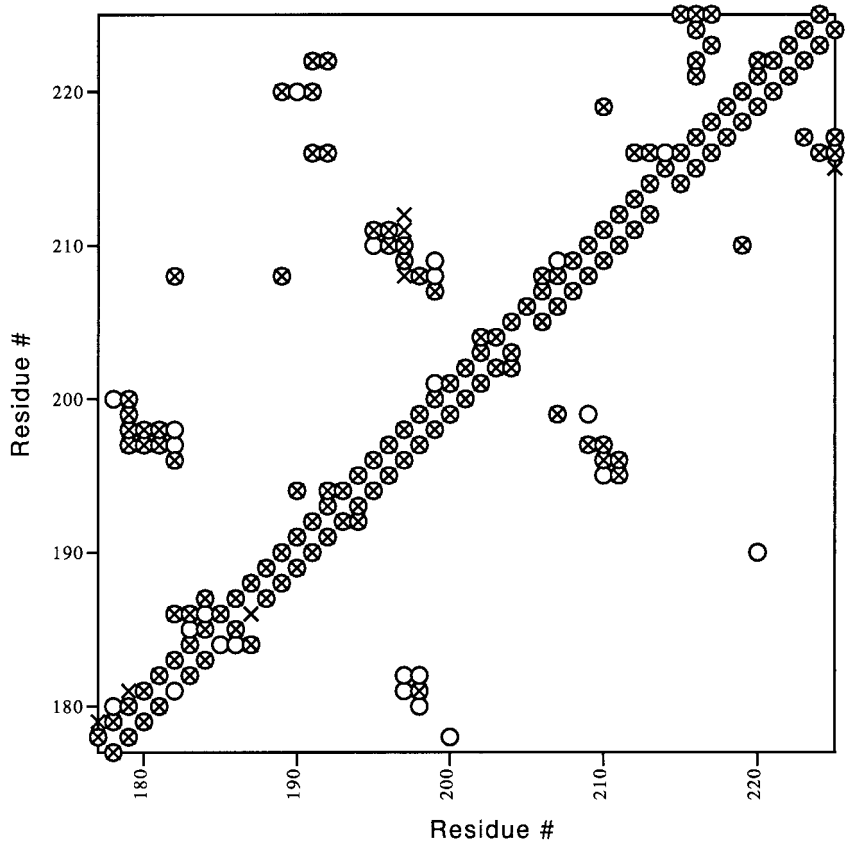

FIG. 1. Diagonal map of the interresidue NOEs for both heregulin-α and HT1. Points above the diagonal represent an NOE between any two protons in different residues. Below the diagonal, only backbone NOE's are plotted. O's are used to denoted the NOEs observed for heregulin-α and X's are used for HT1. Only the results from residues 177-225 are displayed.

suppression was performed using a watergate pulse sequence (8) for the HT1 mutant.

The sequential proton assignments for both proteins were obtained using standard homonuclear techniques (9). The chemical shift of water was assigned at 4.84 ppm at 8°C and 4.63 ppm at 25°C. The chemical shifts are reported for 8°C at pH 3.1.

The slowly exchanging amide protons were identified using the following means. Approximately 4 mg of the protein dissolved in H_2O, pH 3.1, was lyophilized over night. The next day the protein was taken up in 1 ml of 99% D_2O and kept at room temperature for 1 hr. The sample was again lyophilized and dissolved the following day in 99.996% D_2O. The pH was not checked. After an experimental setup that lasted approximately one hour, the slowly exchanging amides were identified using a short mixing clean TOCSY. 512 T_1 increments were collected over a 20 hr period.

Structural constraints. Data for the native protein was analyzed as describe by Adler et al. (7) with the following exceptions. First, there was no attempt to quantify the NOE peak intensities. All NOEs were assigned an initial upper bound of 5Å. The upper bound was then increased to compensate for ambiguities in the stereospecific assignments. Second, hydrogen bond constraints were added for 14 HN's. A constraint was used if and only if there was a backbone to backbone NOE that confirmed the assignment of the hydrogen bond acceptor.

The NOEs for heregulin-α were used as an aid in interpreting the NOEs for the HT1. A back-calculated spectrum was predicted for HT1 using the assigned NOE peaks from heregulin-α. The chemical shifts of the crosspeaks were predict using the sequential assignments of HT1. The back-calculated spectra were then compared to NOESY spectra of HT1 collected with a 200 ms mixing period. The comparisons were made at both 8°C and 25°C. If a well-resolved peak was observed in HT1 spectra at the predicted location, the NOE assignment was accepted. Additional NOE assignments were also made for thirty new crosspeaks between nonsequential residues.

Structure calculations. All structures were generated using the distance geometry package, DGII, of insightII (version 2.3.9, Biosym Technologies, Inc., San Diego, CA). After smoothing the bound matrix using the triangle inequality, the individual structures were embedded and subject to 30,000 steps of simulated annealing at a maximum temperature of 200°K. The resultant structures were minimized by a conjugate gradient using a maximum of 1000 steps. A hundred independent structures were calculated for each protein. The best twenty structures, judged by the residual value of the penalty function, were used for making comparisons.

RESULTS

Solution structure of HRGα. The solution structure of heregulin-α is derived from a total of 465 NOEs, 27 constraints on the angle ϕ, and 14 hydrogen bond constraints. The NOEs have the following breakdown: 58 intraresidue, 234 sequential, 41 medium range [i to i + (2 − 5)] and 132 long range [i to i + (≤6)] NOEs. A diagonal map of the NOEs appears in Fig. 1. None of the twenty structures used for the evaluation had violations greater than 0.3Å. The root mean squared de-

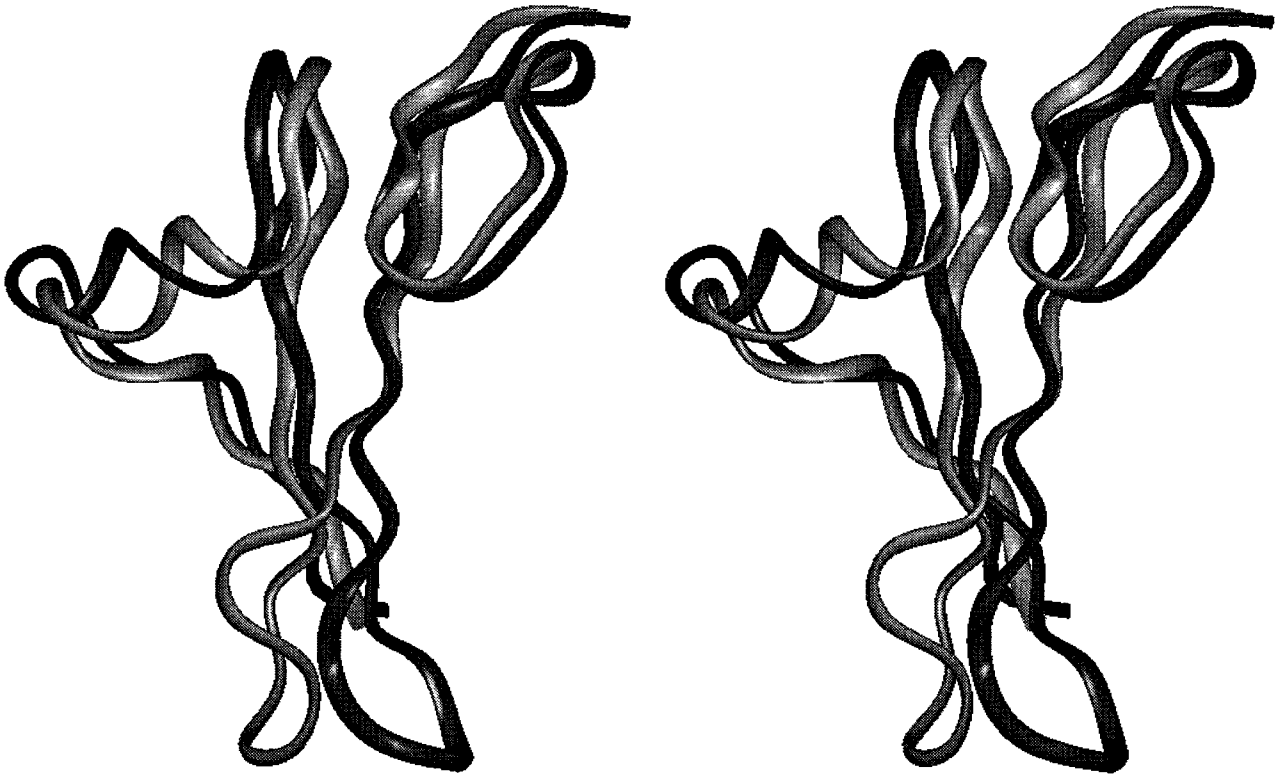

FIG. 2. Comparison of different structures for heregulin-α. Our structure for heregulin-α is shown in dark gray. This structure has the lowest residual penalty function. The structure obtained by Jacobsen *et al.* (5) is shown in light gray (1HAF). The orientation approximates the same position of Fig. 10 of Jacobsen *et al.* (5). As in Figs. 3 and 4, the figure displays the structural core of the protein, residues 177-225.

viation (RMSd) to the mean structure is 1.0Å for the best determine parts of the backbone. The structure is similar to the published coordinates of two other groups (4, 5). The work of Nagata et al. (4) was performed at pH 6.0, 37°C, with unlabeled protein (deposited in the protein data bank as 1HRE). Jacobsen et al. (5) determined the structure at pH 4.5, 20°C, with ^{15}N enriched protein (deposited as 1HAF).

The three structures for heregulin-α share the same global architecture. The RMSd between our structure and 1HAF (5) is 1.9Å for backbone atoms of residues 179-199 and 207-225. The corresponding figure for 1HRE (4) is 2.7Å. The comparison between 1HAF and 1HRE shows that there is a 2.4 Å difference in the RMSd for these backbone atoms.

A closer examination of the structures (Fig. 2) indicates that there are two significant differences between our structure and 1HAF (5). The first turn of the α-helix, residues 185-189 in the A-loop, is less compact in our structure than corresponding helix in 1HAF (Fig. 3 shows the location of each loop). This can be seen in the upper left hand side of Fig. 2. The structural differences may arise from the observed $^{3}J_{HN\text{-}H\alpha}$ coupling constants for residues 185-188. Our measurements indicate that residues all these had coupling constants greater than 9.0 Hz. This is consistent with a more extend structure. Jacobsen et al. (5) measured coupling constants that were less than 8 Hz for Lys^{185}, Lys^{187}, and Thr^{188}. It is possible that the helix becomes more compact at higher pH when the carboxyl groups of Glu^{184} and Glu^{186} balance out the negative charges of Lys^{185} and Lys^{187}.

The other major difference involves the packing involved C-loop, residues 212-221. Our calculations show that this loop is more closely pacted against the strands of the β-sheet in the B-loop. Again, the changes stem from differences in the data. We assigned a hydrogen bond from the HN of Cys^{210} to the CO of Ala^{219} (Fig. 3). Our experiments showed that the amide of Cys^{210} was protected from solvent exchange. The hydrogen bond acceptor, Ala^{219} CO, was identified from an NOE between Cys^{210} HN of and Ala^{219} $C^{\alpha}H$. The work of Jacobsen et al. (5) also indicates that the HN of Cys^{210}, labeled as Cys^{34}, was protected from solvent exchange. However, no hydrogen bond was assigned to this group.

Similar structural perturbations (data not shown) are seen between our structure and 1HRE (4). The A-loop and C-loop in our structure are more closely aligned with 1HAF (5). Perturbations in other loops of the proteins lie within the accuracy of our measurements.

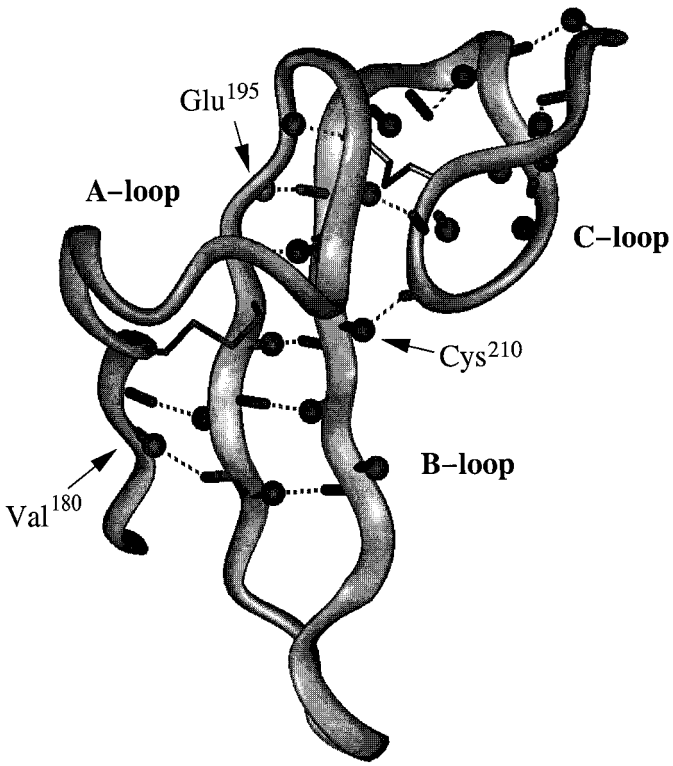

FIG. 3. Slowly exchanging amide protons in heregulin-α. The amide protons are shown as spheres connected by a rod to the nitrogen. Carbonyls that have been identified as the hydrogen bond acceptors are shown as solid rods. A dotted line is used to depict the hydrogen bond. The two visible disulfides are shown as thin rods. Labels are shown for the A-, B-, and C-loops. The molecule is rotated by approximately 45° to the right on the vertically axis compared to Fig. 2.

Solution structure determination of HT1 and comparison to HRGα. The structure of HT1 is derived from a total of 385 NOEs with the following distribution: 46 intraresidue, 195 sequential, 33 medium range [i to i + (2 − 5)] and 111 long range [i to i + (≤6)] NOEs. In addition there are 12 hydrogen bond constraints. Since the $^{3}J_{HN\text{-}H\alpha}$ coupling constants were not quantified, there are no restraints on ϕ.

Comparisons between the NOE assignments of HT1 and HRGα show that the two data sets are very similar (Fig. 1). HRGα has 424 NOEs in the well-ordered parts of the protein, residues 177-225. 344 of these NOEs are also assigned in HT1. 15 NOE peaks are missing in the HT1 spectra, i.e. there should be a resolved NOE crosspeak in the spectrum of HT1 and none is observed. Five of the missing peaks belonged to one of the substituted residues in the N-terminus, Val^{180} → Asn. This asparagine represents a polar substitution for the original hydrophobic valine of HRGα. The more hydrophilic side chain may not be as closely pack against the rest of the protein. All the other missing NOEs involve residues outside the N-terminus. Additionally, 65 NOE crosspeaks from HRGα are not assigned in the HT1 spectra, because the potential crosspeaks are not well resolved. This includes 25 nonsequential NOEs from residues in the N-terminus.

There were 17 slowly exchanging amide protons observed in the HT1 mutant. This compares with 19 observed in the intact protein. The two missing amide protons were Val^{180} → Asn and Glu^{195}. Both these residues are part of the triple stranded β-sheet (Fig. 3). The apparent loss of the slowly exchanging amide from Asn^{180} may simply reflect the higher exchange rate for amide protons in polar residues as compared to hydrophobic residues such as valine. The five other hydrogen bonds in the triple stranded β-sheet are still intact. These include the hydrogen bond between HN of Met^{198} and CO of Asn^{180}. The presence of these five hydrogen bonds strongly indicates that the N-terminal residues still participate in the β-sheet.

Calculations performed with the HT1 constraint set produced a structure that has the same fold as HRGα. There is a measurable increase in disorder for the N-terminus. The RMSd C$^{\alpha}$'s for the three substituted residues, Leu^{179} → Phe, Val^{180} → Asn, and Lys^{181} → Asp, is 0.9Å higher in HT1 than for the corresponding residues in HRGα. These results, however, should not be over interpreted. Much of the increase in scatter can be attribute to loss of 25 NOEs constraints. These NOE peaks are not resolved in the NOESY spectra of HT1 because of the changes in chemical shifts. Therefore, the observed increase in the RMSd reflects the experimental uncertainty and not necessarily any change in conformation.

Our conclusion is that, within the accuracy of our NOE data, there is no detectable differences between the two structures. It must be remember that the structure was solved using homonuclear NMR. Therefore, most of the NOE data comes from the backbone protons that are well-resolved. There is much less information about the location of the amino acid side chains that give poorly resolved crosspeaks in a 2D spectra. There may be significant rearrangements in the side chains in HT1 that have escape detection by these methods.

Fortunately, there is another method available for measuring conformational perturbations. The chemical shifts of the individual protons are sensitive to small changes in their environment. Unfortunately, the information can not be reliably translated into conformation restraints. However, the chemical shift data does yield important qualitative information about perturbations in the structure.

A graphical presentation of the chemical shift data appears in Fig. 4a. The figure was simplified by only displaying the residues where a side chain proton shifted by at least 0.10 ppm. The biggest changes involve the residues in the triple stranded β-sheet. The strongest perturbations are clustered on the left side of the sheet and affect residues Leu^{179}, Lys^{181}, Leu^{209}, and

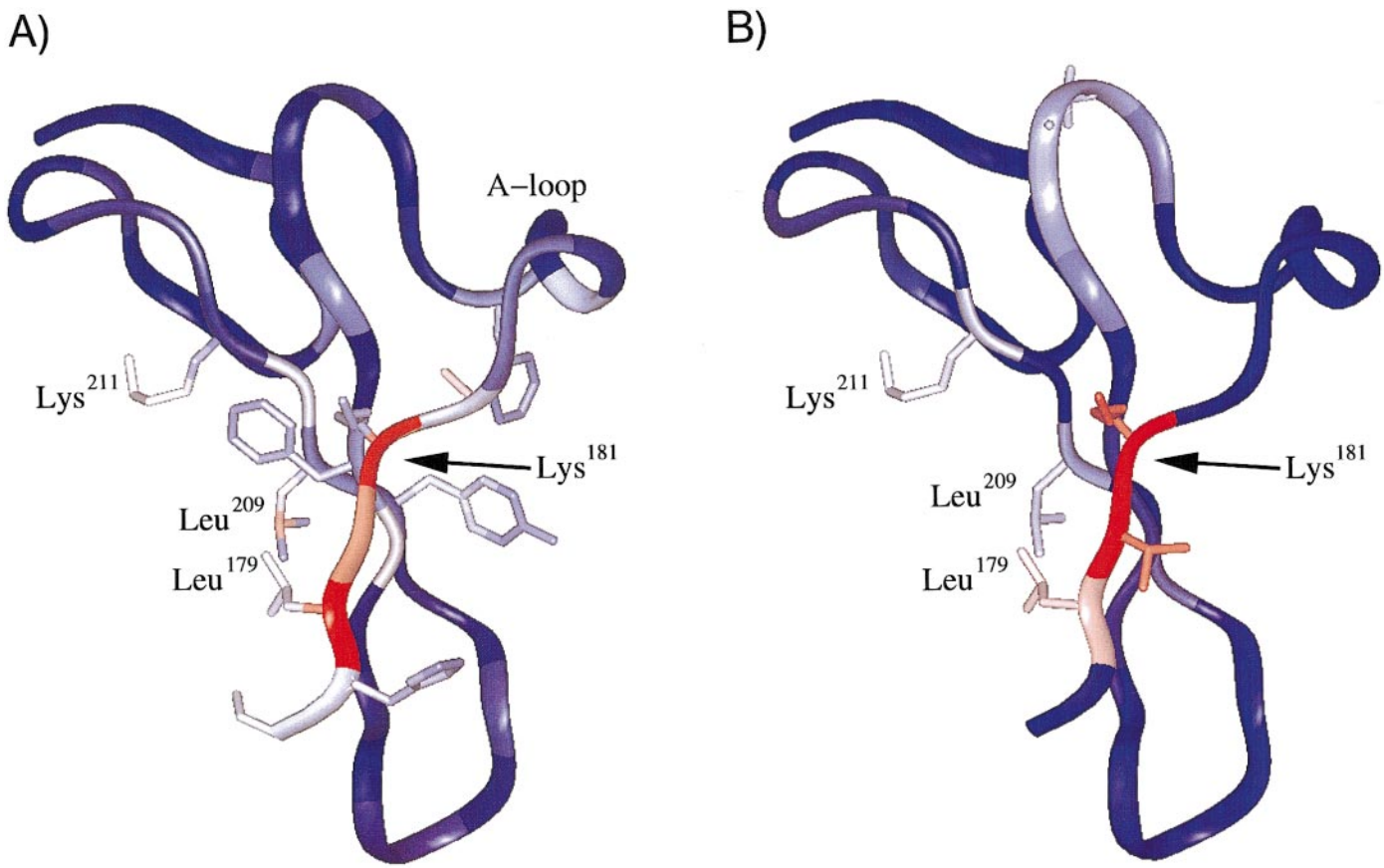

FIG. 4. Comparison of the chemical shift data (A) to the mutation data (B). Panel A displays the changes in chemical shift of homologous atoms in HRGα and HT1. The chemical shifts were first normalized against the values obtained by Bundi and Wüthrich (10) for the amino acids incorporated into unstructured peptides. The color value of the heavy atoms is determined by the average of their attached proton(s) or by the average of the nearest assigned proton(s). The backbone ribbon is colored by the chemical shift of the $C^{\alpha}H$. Color values are assigned as follows: a 0.0 change in ppm is assigned blue, 0.2 ppm is white, and 0.4 ppm or higher is given red. Intermediate values are shaded appropriately. The side chains are shown for residues where at least one side chain proton shifted by 0.10 ppm or more. Panel B displays the information obtained from the homologue scan (1). The individual residues are color coded to show the effect of a mutation on the activity. The colors are assigned based on the Log (K_D^{mut}/K_D^{wt}). Red represents a 1288-fold loss of activity. White represents 36-fold loss of activity. Blue represents either no loss or an increase in activity. Blue is also used if the same residue is found in both HRGα and the mutant protein. Conservative mutations, such as $Arg^{207} \rightarrow$ Lys and $Phe^{216} \rightarrow$ Tyr, are assigned values that are half the original Log (K_D^{mut}/K_D^{wt}). If the mutations involved a significant change in shape but retained the same hydrophobicity and charge, then the color value is assigned at 2/3 of Log (K_D^{mut}/K_D^{wt}). Examples are $Leu^{179} \rightarrow$ Phe and $Leu^{209} \rightarrow$ Ala. Side chains are shown for mutations that reflect at least 10-fold loss of activity. The molecule is rotated on the vertically axis by a half turn compared to Fig. 2.

Lys^{211}. A second cluster of smaller perturbations is seen on the opposite face of the β-sheet. These perturbations extend out to the A-loop. Finally, the side chains of both Ser^{171} and His^{172} show changes in their chemical shifts. However, these chemical shift differences probably reflect the change in the length of the N-terminus and do not necessarily report on any structural perturbations.

It should be noted that the side chains of these proteins are loosely packed and can rotate freely. The experimental data show that the Phe and Tyr side chains have the same chemical shifts for the δ and ϵ protons on both sides of the phenyl ring. If the side chains were fixed in position, then the protons on different sides of the ring would have different shifts. The rapid rotations of these rings average out the differences (this is frequently seen for aromatic residues on the surface of proteins.)

DISCUSSION

The NOE data clearly show that HRGα and HT1 share the same global fold and, within experimental error, the positions of the backbone atoms remain the same. The chemical shift data indicate that the packing of the side chains is changed. However, the data also show that there is a fair amount of flexibility in these side chains. It should be possible for HT1 to adapt the native conformation with little loss in energy. Therefore, the thousand fold reduction in bind affinity of HT1 must stem from the

mutation of residues that form part of the binding epitope and not from any conformational effects of the substitutions. Based upon the sequence information, the three most critical mutations are $Leu^{179} \rightarrow Phe$, $Val^{180} \rightarrow Asn$, and $Lys^{181} \rightarrow Asp$.

Researchers have already established that the N-terminus is critical for the binding of HRGα its receptor (2, 3). Work presented in the previous paper (1) strongly suggest that residues in the B-loop also play a role in the binding epitope. In particular, mutation of $Lys^{211} \rightarrow Asn$ seems to affect the binding. In Fig. 4, the chemical shift data is compared to the results from the homologue scan (1). Fig. 4b shows only results from those mutations that reduced the activity towards the native receptor. Presumably, these residues form the epitope that creates the specific binding site for HRGα. The color values of the residues are proportional to the Log (K_D^{mut}/K_D^{wt}) and have been altered to take into account the affects of conservative mutations. The most brightly colored residues are on the left side of the triple stranded β-sheet (Fig. 4b). Many of these residues are also depicted in Fig. 4a. Four residues standout in both figures: Leu^{179}, Lys^{181}, Leu^{209}, and Lys^{211}. These residues belong to the either HT1 or HE6 mutants (1). The results suggest that there is a good correlation between the chemical shift data from HT1 and the homologue scan results. This in turn suggests that the binding epitope spans across the face of the β-sheet and includes residues in both the N-terminus and the B-loop.

ACKNOWLEDGMENTS

We thank Angela Harris for her help in preparing the HT1 construct. Furthermore, we are grateful for the support given to this work by Drs. Richard N. Harkins and Marc D. Whitlow.

REFERENCES

1. Harris, A., Adler, M., Brink, J., Lin, R., Ferrer, M., Foehr, M., Langton-Webster, B. C., Harkins, R. N., and Thompson, S. A. (1998) *Biochem. Biophys. Res. Commun.* **243,** in press.
2. Barbacci, E. G., Guarino, B. C., Stroh, J. G., Singleton, D. H., Rosnack, K. J., Moyer, J. D., and Andrews, G. C. (1995) *J. Biol. Chem.* **270,** 9585–9589.
3. Chau, B. N., Nandagopla, K., Niyogi, S. K., and Campion, S. R. (1996) *Biochem. Biophys. Res. Commun.* **229,** 882–886.
4. Nagata, K., Kohda, D., Hatanaka, H., Ichikawa, S., Matsuda, S., Yamamoto, Y., Suzuki, A., and Inagaki, F. (1994) *EMBO J.* **13,** 3517–3523.
5. Jacobsen, N. E., Nasrin, A., Sliwkowski, M. X., Reilly, D., Skelton, N. J., and Fairbrother, W. J. (1996) *Biochem.* **35,** 3402–3417.
6. Kline, T. P., Brown, F. K., Brown, S. C., Jeffs, P. W., Kopple, K. D., and Mueller, L. (1990) *Biochem.* **29,** 7805–7813.
7. Adler, M., Seto, M. H., Nitecki, D. E., Lin, J.-H., Light, D. R., and Morser, J. (1995) *J. Biol. Chem.* **270,** 23366–23372.
8. Piotto, M., Saudek, V., and Sklenar, V. (1992) *J. Biomol. NMR* **2,** 661–666.
9. Wüthrich, K. (1986) *NMR of Proteins and Nucleic Acids,* Wiley, New York.
10. Bundi, A., and Wüthrich, K. (1979) *Biopolymers* **18,** 285–298.